Journal of Geodesy (2004) 78: 272–282
DOI 10.1007/s00190-004-0397-y

Journal of Geodesy

The Rudzki inversion gravimetric reduction scheme in geoid determination

S. Bajracharya, M.G. Sideris

Department of Geomatics Engineering, The University of Calgary, 2500 University Drive N.W., Calgary, Alberta, T2N 1N4, Canada
e-mail: bajrachs@ucalgary.ca; Tel.: +1-403-220-4565; Fax: +1-403-284-1980

Received: 28 August 2002 / Accepted: 10 June 2004 / Published online: 20 October 2004

Abstract. Gravimetric reduction schemes play an important role in precise geoid determination, especially in rugged areas. The Rudzki inversion is the only gravimetric reduction scheme that does not change the equipotential surface. The topographical masses above the geoid are inverted into its interior in this scheme. Although the potential of the topography is equal to that of the inverted masses, and thus there is no indirect effect on the geoid using this mass reduction scheme, the attractions of the topography and the inverted topography are not equal. The formulas to compute the attraction due to topographical masses above the geoid and due to inverted masses are studied in planar approximation. One of the most rugged areas in the Canadian Rocky Mountains, which lies between 49°N and 54°N latitude and between 236°E and 246°E longitude, is selected to compute the gravimetric geoid solution using the Rudzki method. It is compared with geoid models based on Helmert's second method of condensation and the residual terrain model (RTM), which are most commonly used in practice, and also with those based on the topographic–isostatic reduction methods of Airy–Heiskanen and Pratt–Hayford. Results show that the Rudzki geoid solution performs as well as the Helmert and RTM geoid solutions (in terms of standard deviation and range of maximum and minimum values) when compared to GPS-leveling data in this test area.

Key words Geoid – Rudzki reduction – indirect effects – Helmert's condensation method – Residual terrain modeling

1 Introduction

The topographical effect is one of the most important components in the solution of the geodetic boundary value problem (BVP), and should be treated properly in the determination of a precise geoid or quasigeoid. The classical solution of the geodetic BVP using Stokes's formula for geoid determination assumes that there are no masses outside the geoid (see e.g. Heiskanen and Moritz 1967). The input gravity anomalies should refer to the geoid, which requires the actual Earth's topography to be regularized in some way. The mathematical and physical treatments of this issue play an important role in the computation of a precise (local or regional) gravimetric geoid solution. There are several reduction techniques, which all differ depending on how these topographical masses outside the geoid are dealt with. In theory, the gravimetric solution for geoid determination using different mass reduction methods should give the same result, provided that the corresponding indirect effect is taken into account properly and consistently (Heiskanen and Vening Meinesz 1958; Heiskanen and Moritz 1967).

The importance of gravimetric mass reduction in quasigeoid determination was first introduced by Pellinen (1962). The specific choice of gravity reduction method depends on the magnitude of its indirect effect, the smoothness and the magnitude of the resulting gravity anomalies, and their associated geophysical interpretation. The complete Bouguer reduction, for example, removes all topographic masses above the geoid producing smooth gravity anomalies, but introduces excessively large indirect effects (see e.g. Heiskanen and Moritz 1967). Topographic–isostatic gravity reductions [e.g. Airy–Heiskanen (AH) and Pratt–Hayford (PH)], on the other hand, remove the topographic masses by shifting them into the interior of the geoid according to some model of isostasy, and they exhibit all the characteristics of a 'good' gravity reduction scheme. These methods introduce indirect effects of the order of several metres, which are much smaller than that of the Bouguer scheme, but still larger than that of Helmert's second method of condensation, and thus have not commonly been used in geoid determination since the late 1970s.

Correspondence to: S. Bajracharya

In Helmert's second method, the topographic masses between the geoid and the Earth's surface are condensed onto the geoid, forming a surface layer. The direct topographic effects and indirect effects using this condensation reduction method have been discussed in the literature (see e.g. Heiskanen and Moritz 1967; Wichiencharoen 1982; Wang and Rapp 1990; Sideris 1990; Heck 1993; and Vanicek and Martinec 1994). The residual terrain modeling (RTM) scheme, which is not a topographic–isostatic reduction but gives anomalies similar to topographic–isostatic anomalies, has been used for almost two decades as a common tool for terrain reduction in geoid computation (Forsberg 1984). The recent studies on Helmert's first method of condensation by Heck (2003) and on topographic–isostatic reductions by Abd-Elmotaal and Kühtreiber (2003), Bajracharya (2003), and Kuhn (2003) can be considered as an exploration of different gravimetric reduction techniques for geoid determination, in addition to the RTM and Helmert's second method of condensation.

An interesting method in gravimetric reduction is the Rudzki inversion scheme (Rudzki 1905; Heiskanen and Vening Meinesz 1958; Heiskanen and Moritz 1967). Rudzki postulated his theory of gravimetric reduction in such a way that the potential of topographical masses above the geoid is equal to that of inverted topographical masses inside the geoid. Apart from Rudzki's own original work on this reduction scheme, it has not been used for geoid determination. However, emphasis on using this gravimetric scheme was given by Lambert (1930). This reduction method is purely mathematical and has no associated geophysical meaning, which is not as important in geoid determination as in geophysics.

The purpose of this paper is to present the gravitational integrals used in Rudzki's inversion scheme and compute the Rudzki geoid in one of the most rugged areas in the Canadian Rocky Mountains. A comparative analysis of the Rudzki geoid solution with those based on Helmert's second method of condensation and the RTM, which are most commonly used in practice, and also those based on the topographic–isostatic reduction methods of AH and PH, is performed.

2 Gravitational integrals for the Rudzki inversion scheme

In potential theory, a point Q' (see Fig. 1) can be regarded as an inversion of point Q on a sphere of radius R, if both points are on the same radial from the center of the sphere and if the radius of the sphere is the geometric mean of their distances r and r' from the center (Kellogg 1929). Hence the term *inversion* is used in Rudzki's gravimetric method. The point Q' is also known as the mirror image of Q. Here, the geoid is approximated by a sphere of radius R. Not only single points can be inverted (or mirrored) into the geoid using this inversion theory, but also whole topographical masses, as shown in Fig. 1. The condition of the inversion on the sphere can be expressed as (MacMillan 1958)

$$\frac{r}{R}=\frac{R}{r'}\ ;\ \mathrm{d}r=\frac{R^2}{r'^2}\mathrm{d}r' \tag{1}$$

An algebraic negative sign in the second part of Eq. (1) is eliminated for convenience, assuming that when r changes to $r+\mathrm{d}r$, the corresponding r' will move to $r'-\mathrm{d}r'$, thus making both $\mathrm{d}r$ and $\mathrm{d}r'$ of the same sign.

The main condition in Rudzki's inversion method is that the indirect effect on the geoid is zero. The gravitational potential at point P_o on the geoid (and for any points on the geoidal surface) due to mass element $\mathrm{d}m$ at point Q is equal to that of the inverted mass element $\mathrm{d}m'$ at point Q', which can be expressed as

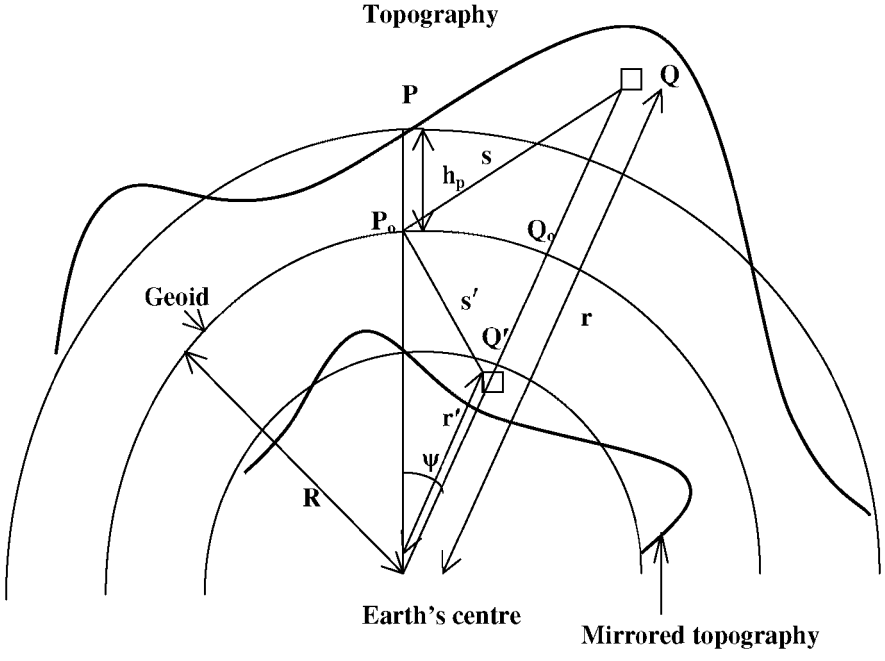

Fig. 1. Geometry of Rudzki reduction in spherical approximation

$$\Delta T = T - T' = 0; \quad T = T' \tag{2}$$

where ΔT is the difference between the gravitational potential T of the topographical masses and that of the inverted topographical masses, T'. The differential potential $\mathrm{d}T$ at point P_o on the geoidal surface due to the topographic mass element $\mathrm{d}m$ and the differential potential $\mathrm{d}T'$ at the same point due to the mirrored topographical mass element $\mathrm{d}m'$ can be expressed as

$$\begin{aligned} \mathrm{d}T &= G\frac{\mathrm{d}m}{s} = \frac{G\rho r^2 \cos\varphi \mathrm{d}r\mathrm{d}\lambda\mathrm{d}\varphi}{\sqrt{(r^2 + R^2 - 2rR\cos\psi)}}; \\ \mathrm{d}T' &= G\frac{\mathrm{d}m'}{s'} = \frac{G\rho' r'^2 \cos\varphi \mathrm{d}r'\mathrm{d}\lambda\mathrm{d}\varphi}{\sqrt{(r'^2 + R^2 - 2r'R\cos\psi)}} \end{aligned} \tag{3}$$

where G is the universal gravitational constant; (r, φ, λ) and (r', φ, λ) are the spherical coordinates of the topographical mass element of density ρ and the mirrored topographical mass element of density ρ', respectively, s and s' are the radial distances between point P_o and the mass elements, and ψ is the angle formed by the radius vectors pointing from the Earth's geocenter to point P_o and the mass elements. Applying the condition of the inversion on the sphere from Eq. (1) and the condition of Rudzki's scheme from Eq. (2) to Eq. (3), the following equation can be obtained:

$$\rho' = \left(\frac{r}{R}\right)^5 \rho = \left(1 + \frac{z}{R}\right)^5 \rho; \quad \rho' = \left(\frac{R}{r'}\right)^5 \rho = \left(\frac{1}{1 - z'/R}\right)^5 \rho \tag{4}$$

where $z = r - R$ is the height Q_oQ of topographical mass element and $z' = R - r'$ is the height $Q'Q$ of the inverted mass element (Fig. 1). Equation (4) provides the fundamental relationship between the *in situ* topographical density and the density of the mirrored topographical masses below the geoid in Rudzki's gravimetric scheme. It shows that the ratio of the densities of the mirrored and topographical masses is proportional to the fifth power of either the ratio of the radial distance of the topographical masses to the radius of the Earth or the ratio of the radius of the Earth to the radial distance of the inverted masses. If we take a mass element at the top of Mount Everest, the density of the mirrored topographical mass element will change by 0.7% of the standard Earth's mean topographical density of 2670 kg/m^3.

Similarly, from Eqs. (1), (2), and (3), the following formula can be obtained:

$$\mathrm{d}m' = \frac{R}{r}\mathrm{d}m \tag{5}$$

which shows that the shifting of topographical masses into the geoid by mirrored masses introduces a slight mass change. The inverted topographical masses are slightly smaller than the topographical masses. It is obvious from Eq. (5) that if the mass element is near the geoidal surface, these two types of masses become nearly equal and the height of the topographical mass element will be nearly equal to the depth of the inverted masses below the geoid. For a planar model of the geoid (see Fig. 2), we can obtain the following conditions by letting $R \to \infty$ in Eqs. (4), (5), and (1):

$$\rho' = \rho; \quad \mathrm{d}m' = \mathrm{d}m; \quad z' = z \tag{6}$$

In the planar model, the potential T_p of the topographical masses outside the geoid at a point P can be

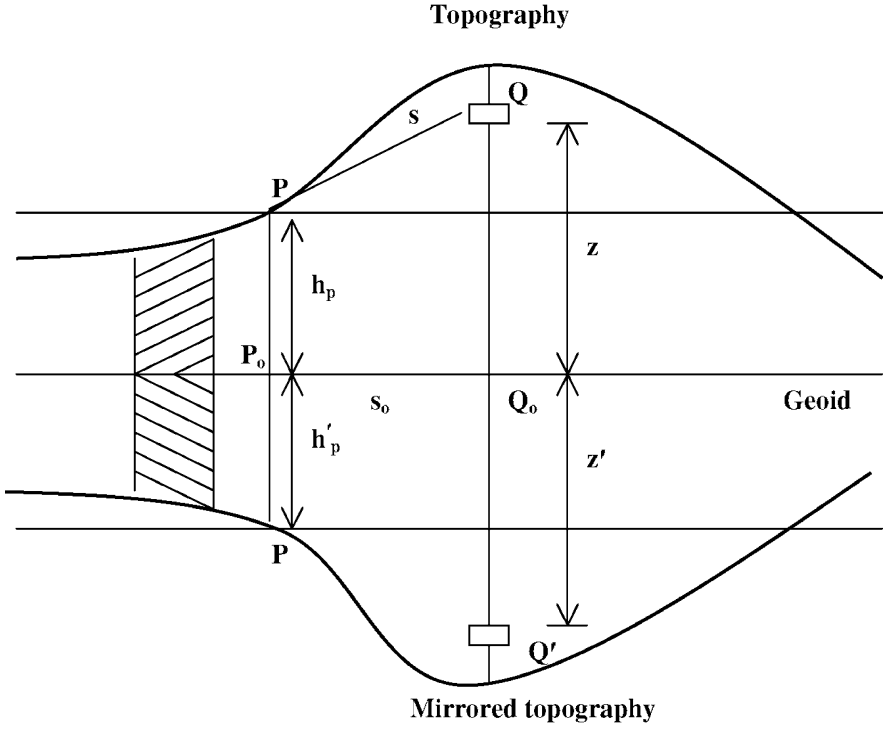

Fig. 2. Geometry of the Rudzki reduction in planar approximation

expressed by the sum of two integrals which represent the potential of the regular part (Bouguer plate of thickness h_p) and the irregular part (rough terrain) of the topography as follows:

$$T_p = G\rho \iint_E \int_0^{h_p} \frac{1}{s}\, dE dz + G\rho \iint_E \int_{h_p}^{h} \frac{1}{s}\, dE dz \tag{7}$$

$$s = \left[s_o^2 + (z - h_p)^2\right]^{1/2}; \quad s_o = \left[(x - x_p)^2 + [(y - y_p)^2\right]^{1/2} \tag{8}$$

where dE is a differential area, and (x_p, y_p, z_p) and (x, y, z) are the coordinates of the computation and running point in a planar system, respectively. The following expression can be obtained by introducing the gravitational potential of a homogenous circular cylinder of radius a and height h_p (when the regular part of the topography is represented by a homogenous cylinder; Heiskanen and Moritz 1967) into the first term of Eq. (7)

$$T_p = \pi G\rho[-h_p^2 + h_p\sqrt{a^2 + h_p^2} + a^2 \ln \frac{(h_p + \sqrt{a^2 + h_p^2})}{a} + G\rho \iint_E \int_{h_p}^{h} \frac{1}{s}\, dE dZ \tag{9}$$

The gravitational attraction of all the topographical masses above the geoid at a point P can also be expressed as a sum of the attractions of the regular and irregular parts of the topography as:

$$A_p = 2\pi G\rho[h_p + a - \sqrt{a^2 + h_p^2}] - G\rho \iint_E \left(\frac{1}{s_o} - \frac{1}{\left[s_o^2 + (h - h_p)^2\right]^{1/2}}\right) dE \tag{10}$$

This attraction due to the topographical masses of an infinite Bouguer plate ($a \to \infty$) can be expressed as

$$A_p = 2\pi G\rho h_p - G\rho \iint_E \left(\frac{1}{s_o} - \frac{1}{\left[s_o^2 + (h - h_p)^2\right]^{1/2}}\right) dE \tag{11}$$

which represents the gravitational attraction due to all topographical masses above the geoid. Equation (11) is common in all gravimetric reductions since the topographical masses above the geoid should be removed completely before applying compensation (condensation or inversion) below the geoid.

The expression for the gravitational attraction at a point P on the topographical surface due to the mirrored topographical masses can also be obtained as a sum of the gravitational attraction due to the regular and irregular parts of the inverted topography as

$$A'_p = 2\pi G\rho' h'_p - G\rho' \iint_E \left(\frac{1}{\left[s_o^2 + (h_p + h'_p)^2\right]^{1/2}} - \frac{1}{\left[s_o^2 + (h_p + h')^2\right]^{1/2}}\right) dE \tag{12}$$

The expression for direct topographical effect on gravity, which is equal to the difference between the gravitational attraction due to all topographical masses above the geoid and that due to the mirrored topographical masses inside the geoid in Rudzki's scheme, can be obtained from Eqs. (6), (11), and (12) as

$$\delta A = A_p - A'_p = G\rho \iint_E \left(\frac{1}{\left[s_o^2 + (h - h_p)^2\right]^{1/2}} - \frac{1}{s_o} + \frac{1}{\left[s_o^2 + (2h_p)^2\right]^{1/2}} - \frac{1}{\left[s_o^2 + (h_p + h)^2\right]^{1/2}}\right) dE \tag{13}$$

In Eq. (13), it is obvious that the attractions due to the regular parts of the topographical and the mirrored topographical masses are equal and thus cancel out. The direct topographical effect on gravity in this Rudzki reduction scheme is the difference between the attraction due to the irregular part of the topography and that of the mirrored topography evaluated at a point P on the surface of the Earth.

3 Computational formulas for geoid determination

The global geopotential model, local gravity information, and digital terrain model loosely represent the low-, medium-, and high-frequency parts of the gravity signal, respectively. Gravimetric geoid computation is carried out using the remove–compute–restore (RCR) technique in this investigation for all gravity reduction methods in planar approximation. First, the gravity anomalies are reduced in a remove step using a mass reduction scheme to formulate boundary values on the geoid, which—when the vertical gradient of gravity is approximated by the vertical gradient of normal gravity—can be expressed as

$$\Delta g = \Delta g_F - \Delta g_T - \Delta g_{GM} \tag{14}$$

where Δg_F is the free-air (FA) anomaly, Δg_T is the direct topographical effect on gravity in each reduction method used, and Δg_{GM} is the reference gravity anomaly from a global geopotential model. The indirect effect on gravity, which reduces gravity anomaly from the co-geoid to the geoid, should be added in Eq. (14) for Helmert's second method of condensation and the topographic–isostatic mass reduction schemes, and can be expressed using the simple, linear free-air gradient (Heiskanen and Moritz 1967)

$$\delta g = 0.3086 N_{\text{ind}} \text{ mGal} \tag{15}$$

The direct topographical effect on gravity Δg_{T} in Eq. (14) for each mass reduction scheme can be expressed as

$$\Delta g = A - A_{(\text{Inv,Cond,Comp,Ref})} \tag{16}$$

where A is the attraction of all topographic masses above the geoid and $A_{(\text{Inv,Cond,Comp,Ref})}$ represents the attraction of either the inverted topographical masses, the condensed masses, the compensated masses, or the reference topographic masses for the Rudzki, Helmert's second method of condensation, AH or PH, and RTM reduction schemes, respectively. The two components on the right-handside of Eq. (16) can be expressed for each reduction scheme as follows:

$$A = G\rho \iint_E \int_0^h \frac{(h_{\text{p}} - z)}{s^3(x_{\text{p}} - x, y_{\text{p}} - y, h_{\text{p}} - z)} \, \text{d}x \, \text{d}y \, \text{d}z$$

$$A_{\text{Inv}} = G\rho \iint_E \int_{-h}^0 \frac{(h_{\text{p}} - z)}{s^3(x_{\text{p}} - x, y_{\text{p}} - y, h_{\text{p}} - z)} \, \text{d}x \, \text{d}y \, \text{d}z$$

$$A_{\text{Comp(Airy)}} = G\Delta\rho \iint_E \int_{-T-t}^{-T} \frac{(h_{\text{p}} - z)}{s^3(x_{\text{p}} - x, y_{\text{p}} - y, h_{\text{p}} - z)} \, \text{d}x \, \text{d}y \, \text{d}z$$

$$A_{\text{Comp(Pratt)}} = G\Delta\rho \iint_E \int_{-D}^0 \frac{(h_{\text{p}} - z)}{s^3(x_{\text{p}} - x, y_{\text{p}} - y, h_{\text{p}} - z)} \, \text{d}x \, \text{d}y \, \text{d}z$$

$$A_{\text{Ref}} = G\Delta\rho \iint_E \int_0^{h_{\text{ref}}} \frac{(h_{\text{p}} - z)}{s^3(x_{\text{p}} - x, y_{\text{p}} - y, h_{\text{p}} - z)} \, \text{d}x \, \text{d}y \, \text{d}z \tag{17}$$

where h and h_{ref} are the (above the geoid) height of the running point and the reference height of the running point, respectively; $\Delta\rho$ is the density contrast between the Earth's crust and the upper mantle in the AH model and the difference between standard crustal density and the actual density in the PH model, and it can be given as (Heiskanen and Meinesz 1958)

$$\begin{aligned} \Delta\rho_{(\text{Airy})} &= \rho_{\text{m}} - \rho = \frac{h\rho}{t}; \\ \Delta\rho_{(\text{Pratt})} &= \rho - \rho_{\text{r}} = \frac{h}{D+h}\rho \end{aligned} \tag{18}$$

where ρ_m and ρ_r are the density of the upper mantle and the actual crust density, respectively; D, T, and t are the depth of compensation for the PH model, the normal crust thickness for the AH model, and the root depth in the AH model, respectively. The second term on the right-hand side of Eq. (11), the terrain correction, represents the direct topographical effect on gravity in Helmert's second method of condensation since it is equal to the difference between the attraction of the topography computed on the surface of the topography and the attraction due to the condensed masses computed on the geoid. The integrals in Eq. (17) can be numerically integrated using rectangular prisms with the computation point coinciding with the origin of the coordinate system (Nagy 1966)

$$A_{\text{T}} = G\rho \Big| \Big| x \ln(y + r) + y \ln(x + r) - z \arctan \frac{xy}{zr} \Big|_{x_1}^{x_2} \Big|_{y_1}^{y_2} \Big|_{z_1}^{z_2} \tag{19}$$

where the coordinates x_1, x_2, y_1, y_2, z_1, and z_2 represent the corners of a prism.

The total geoid obtained from the restore step can be expressed as

$$N = N_{\text{GM}} + N_{\Delta g} + N_{\text{ind}} \tag{20}$$

where N_{GM} denotes the long-wavelength part of the geoid obtained from a geopotential model, $N_{\Delta g}$ represents the residual geoid obtained by using Δg from Eq. (14) in Stokes's formula, and N_{ind} is the indirect effect on the geoid, which depends on the mass reduction scheme used. Stokes's integral formula with the spherical kernel by the one-dimensional fast Fourier transform (1D-FFT) algorithm is used in this paper (Haagmans et al. 1993). The formulas for the computation of Δg_{GM} and N_{GM} are given in Heiskanen and Moritz (1967). The indirect effect on the geoid, in Eq. (20), can be computed from Bruns's formula as follows:

$$N_{\text{ind}} = \frac{\Delta T}{\gamma} \tag{21}$$

where ΔT is the change in the potential at the geoid, which depends on the reduction method used and can be expressed as

$$\Delta T = T - T_{(\text{Inv, Cond, Comp})} \tag{22}$$

where T is the gravitational potential of the actual topographical masses and $\text{T}_{(\text{Inv,Cond,Comp})}$ represents the potential of the inverted, compensated, or condensed masses for the Rudzki, Helmert, and AH or PH reduction schemes, respectively. The term ΔT in Eq. (22) is zero for the Rudzki inversion scheme since the potential of the topography is equal to that of the inverted topography, as given by Eq. (2). The potentials of the topographical masses and the compensating masses for the AH and PH models can be expressed respectively as

$$T = G\rho \iint_E \int_0^{h(x,y)} \frac{1}{s(x_{\text{p}} - x, y_{\text{p}} - y, h_{\text{p}} - z)} \, \text{d}x\text{d}y\text{d}z$$

$$T_{\text{Comp (Airy)}} = G\Delta\rho \iint_E \int_{-T-t}^{-T} \frac{1}{s(x_{\text{p}} - x, y_{\text{p}} - y, h_{\text{p}} - z)} \text{d}x\text{d}y\text{d}z$$

$$T_{\text{Comp (Pratt)}} = G\Delta\rho \iint_{E} \int_{-D}^{0} \frac{1}{s(x_p - x, y_p - y, h_p - z)} \, dx dy dz \tag{23}$$

The integrals in Eq. (23) can also be numerically integrated using rectangular prisms with the computation point coinciding with the origin of the coordinate system (Nagy 1966)

$$T = G\rho \Big| \Big| \Big| xy \ \ln(z + r) + xz \ln(y + r) + yz(x + r) - \frac{x^2}{2} \tan^{-1}\left(\frac{yz}{xr}\right) - \frac{y^2}{2} \tan^{-1}\left(\frac{xz}{yr}\right) - \frac{z^2}{2} \tan^{-1}\left(\frac{xy}{zr}\right) \Big|_{x_1}^{x_2} \Big|_{y_1}^{y_2} \Big|_{z_1}^{z_2} \tag{24}$$

The indirect effect on the geoid for Helmert's second method of condensation can be obtained in planar approximation as (Wichiencharoen 1982)

$$N_{\text{ind}} = -\frac{\pi G\rho}{\gamma} h_p^2 - \frac{G\rho}{6\gamma} \iint_{E} \frac{h^3 - h_p^3}{s_o^3} \, dx dy \tag{25}$$

The RTM reduction method gives the quasigeoid, and the restored effect on the geoid due to the removal of topography according to this model is (Forsberg 1984)

$$N_{\text{res-eff}} = \frac{G\rho}{\gamma} \iint_{h_{\text{Ref}}} \int^{h} \frac{1}{s} \, dx dy dz = \frac{G\rho(h - h_{\text{ref}})}{\gamma} \iint \frac{1}{s_o} dx dy \tag{26}$$

The separation between quasigeoid and geoid can be computed from (Heiskanen and Moritz 1967)

$$\zeta - N = -\frac{\bar{g} - \bar{\gamma}}{\bar{\gamma}} h \approx \frac{\Delta g_B}{\bar{\gamma}} h \tag{27}$$

where $\bar{g}, \bar{\gamma}$ and Δg_B represent the mean gravity, mean normal gravity, and the Bouguer anomaly, respectively.

4 Numerical tests and comparative analysis

One of the most rugged areas in the Canadian Rocky Mountains, bounded by latitude between 49° N and 54° N and longitude between 236° E and 246° E, is selected to compute different gravimetric geoid solutions with the gravimetric reductions presented in the previous sections. A total of 9477 measured gravity values are used for this test, the distribution of which is shown in Fig. 3. The normal gradient of 0.3086 mGal/m is used for the computation of free-air anomalies and the standard constant topographical density of 2670 kg/m^3 is assumed. A digital terrain model with 6 arc-second grid resolution is used in the computations (Fig. 4). The maximum elevation in the test area is 3937 m (mean 1396 m; standard deviation ± 543 m). The attraction of

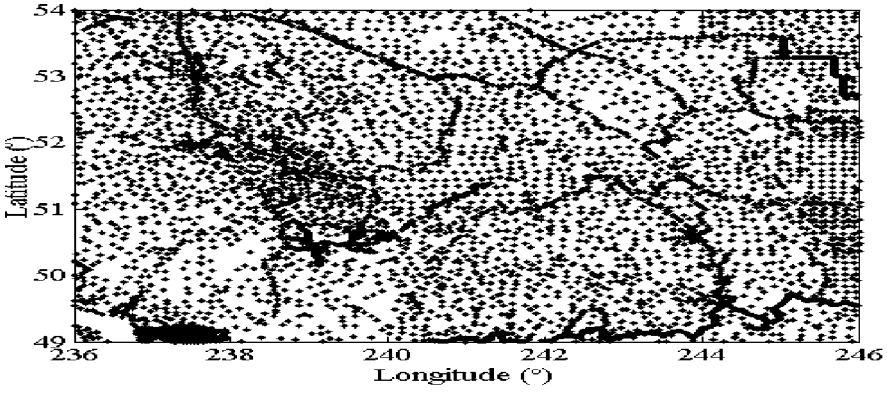

Fig. 3. The distribution of gravity points in the test area

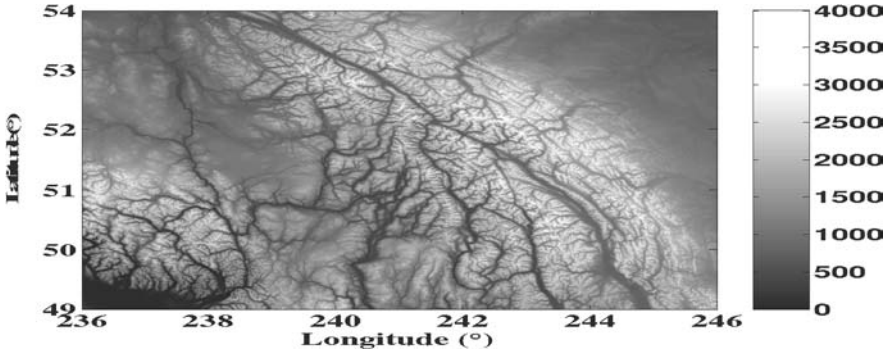

Fig. 4. The digital terrain model in the test area (m)

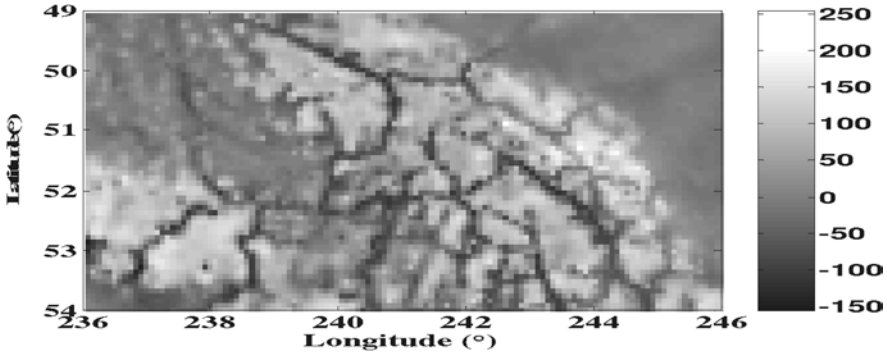

Fig. 5. Helmert anomalies (mGal)

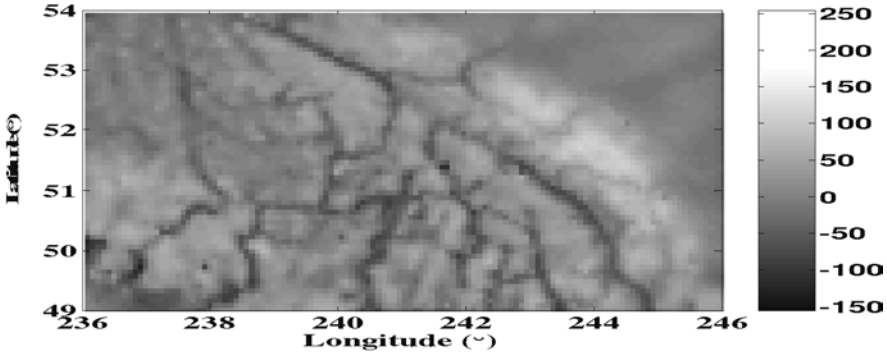

Fig. 6. Rudzki anomalies (mGal)

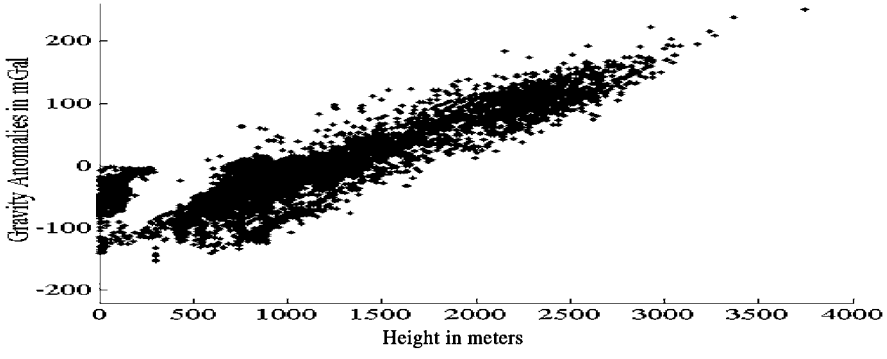

Fig. 7. Correlation between helmert anomalies and topography

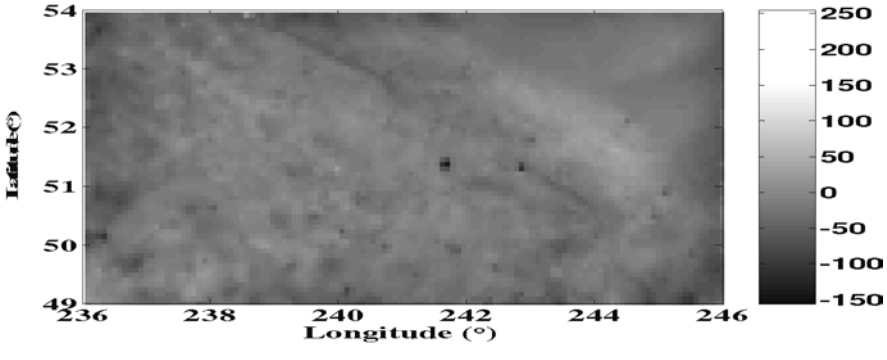

Fig. 8. Airy-Heiskanen topographic-isostatic anomalies (mGal)

the topography, the attraction of the compensating masses, and the attraction of the inverted masses are computed using a radius of 300 km around the computation point. The reference gravity field is computed from the EGM96 geopotential model (Lemoine et al. 1998) complete to degree and order 360. The compensation depth for the PH model is taken as 100 km, while the normal crust thickness for the AH model is assumed equal to 30 km. The density contrast between the Earth's crust and the upper mantle is taken equal to 600 kg/m^3 for this test.

The statistics of the reduced gravity anomalies for different gravimetric reductions are presented in Table 1. The values in parentheses show the statistics of the

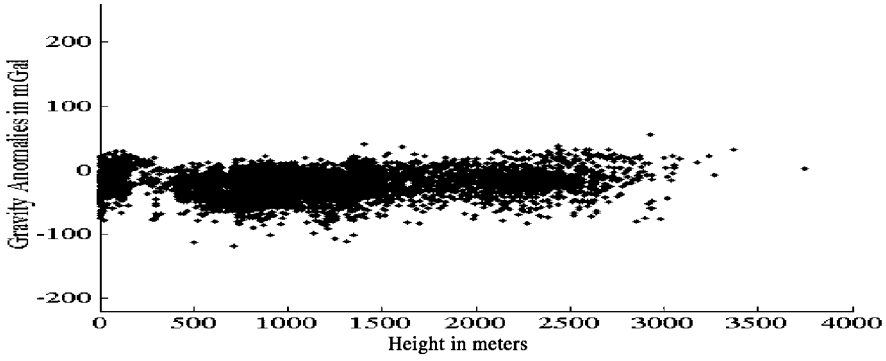

Fig. 9. Correlation between Airy-Heiskanen anomalies and topography

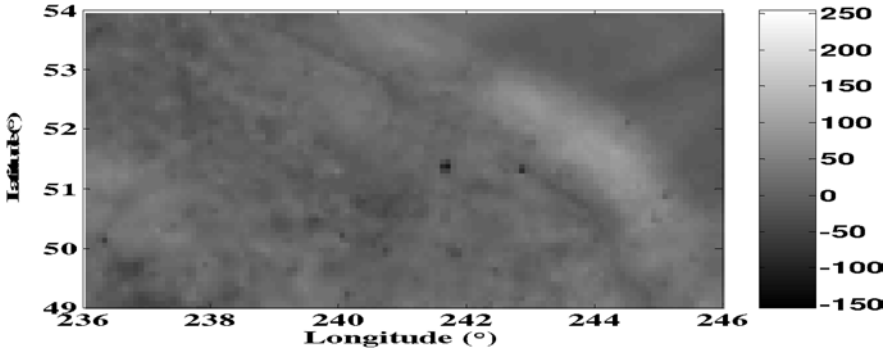

Fig. 10. Residual Terrain Model anomalies (mGal)

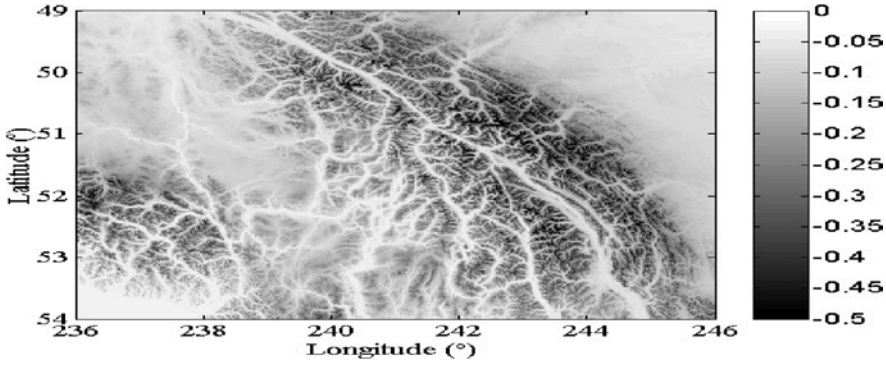

Fig. 11. Indirect effect on the geoid for Helmert's scheme (m)

reduced gravity anomalies when the EGM96 component of the gravity signal is removed. The higher the mountains in the test area, the more negative the values of the Bouguer anomalies are. These large negative Bouguer anomalies suggest that the topographic masses of the Rocky Mountains are compensated according to some models of isostasy.

The Rudzki anomalies fluctuate between a maximum value of 124 mGal and a minimum value of −122 mGal. The maximum and minimum values are seen at stations in high mountains and low valleys, respectively. The statistics of Rudzki, FA, and Helmert anomalies look similar compared to those of the topographic–isostatic anomalies. However, the range of the maximum and minimum values and the standard deviation of Rudzki anomalies are smaller than those of FA and Helmert anomalies. Figures 5 and 6 show the Helmert and Rudzki anomalies. The correlation of the Rudzki and FA anomalies with topography is as strong as that of the Helmert anomalies (Fig. 7).

The topographic–isostatic anomalies using the AH and PH models show nearly the same statistics. These reductions show the best statistics in terms of the standard deviation and the range of maximum and minimum values compared to all reduction methods used in this investigation. Figure 8 shows the AH anomalies. The small difference in the statistics between these two sets of topographic–isostatic anomalies indicates that the attraction of compensating masses using AH and PH models is nearly equal. The correlation of the PH anomalies with the topography looks similar to that of the AH anomalies (Fig. 9), which is much smaller compared to that of other reduction schemes. The RTM anomalies (Fig. 10) exhibit statistics very close to those of AH and PH anomalies.

The statistics of the reduced gravity anomalies in Table 1 show that the standard deviation and the range of maximum and minimum values decrease for Rudzki, FA, Helmert, and RTM anomalies, but increase for Bouguer, AH, and PH anomalies. It is not theoretically

Table 1. The statistics of gravity anomalies (mGal)[a]

Reduction scheme	Max	Min	Mean	Standard deviation
Free air	166.38 (125.47)	−183.58 (−185.77)	−22.39 (−16.53)	50.71 (44.03)
Bouguer	−5.52 (26.61)	−212.87 (−261.30)	−110.08 (−104.23)	43.62 (64.21)
Helmert (Faye)	251.56 (214.65)	−152.67 (−155.74)	−15.06 (−9.20)	58.22 (50.15)
Airy–Heiskanen	49.86 (65.38)	−118.83 (−136.98)	−25.14 (−19.29)	18.54 (28.41)
Pratt–Hayford	49.86 (62.80)	−107.58 (−144.13)	−29.78 (−23.93)	18.05 (29.59)
RTM	115.45 (67.59)	−89.91 (−78.29)	−0.57 (5.20)	23.49 (15.29)
Rudzki	123.69 (77.04)	−122.34 (−118.16)	−17.38 (−11.54)	35.85 (24.22)

[a]Values in parentheses are reduced gravity anomalies.

correct to use EGM96 to subtract the long-wavelength component for all gravimetric reduction schemes. EGM96 is nominally based on FA anomalies, and therefore either a geopotential model corresponding to each reduction scheme should be used, or the corresponding correction for each reduction method should be applied to the coefficients (also see Kuhn 2003). However, it is difficult in practice to create geopotential models based on each reduction scheme.

The indirect effect on gravity for Helmert, AH, and PH models is considered before applying Stokes's formula for these reductions. The statistics of the indirect effects on gravity and the geoid are given in Table 2. The indirect effect on gravity for Helmert's method is very small (sub-mGal), while that of the PH topographic–isostatic reduction reaches a maximum of 3 mGal. The indirect effect on geoid undulations for the PH reduction changes the geoid by nearly 10 m, while that for Helmert's method changes the geoid by only 47 cm. The indirect effects on gravity and the geoid for the AH and PH models have similar statistics. Figures 11 and 12 show the indirect effect on the geoid for Helmert's second method of condensation [Eq. (25)] and the PH model. The maximum indirect effect for all reductions is seen in the mountainous regions. The restored terrain effect on the quasigeoid for the RTM reduction reaches nearly 1 m.

Table 2. Indirect effects on gravity (mGal) and on geoid undulation (m)

Geoid model	Indirect effect	Max	Min	Mean	Standard deviation
Helmert	gravity	0.26	0.00	0.04	0.03
	geoid	0.01	−0.47	−0.12	0.08
Pratt–Hayford	gravity	3.08	0.18	1.35	0.75
	geoid	9.97	0.59	4.36	2.41
Airy–Heiskanen	gravity	2.61	0.09	1.04	0.64
	geoid	8.46	0.31	3.36	2.06
RTM (restrored terrain effect)	quasigeoid	1.07	−1.03	−0.33	0.46

The 258 GPS benchmarks available in the test area (Fig. 13) are used as control for estimating the accuracy of the gravimetric geoid solutions. There are no GPS-leveling points above the elevation of 2000 m. A four-parameter trend surface is applied to fit the gravimetric geoid solutions to the GPS-leveling. The statistics of the differences between the gravimetric geoid undulations and GPS-leveling, before and after the fit, are given in Table 3. The gravimetric geoid solution based on Rudzki's reduction shows almost the same differences as the RTM and Helmert methods in terms of standard deviation and the range of maximum and minimum values after the fit. However, it is interesting that the absolute magnitudes of maximum, minimum, and mean values of the difference between the Rudzki gravimetric solution and GPS-leveling before fit are the smallest, and those based on topographic-isostatic gravimetric solutions of AH and PH models are the largest. As mentioned in the earlier paragraph, the main reason for this large bias is due to the use of EGM96, which is based on FA coefficients. These biases are removed by the fit to the GPS-leveling data, and the range of maximum and minimum values for these models becomes nearly the same as for the Rudzki, Helmert, and RTM methods. However, their standard deviation is 6 cm bigger than that for other methods.

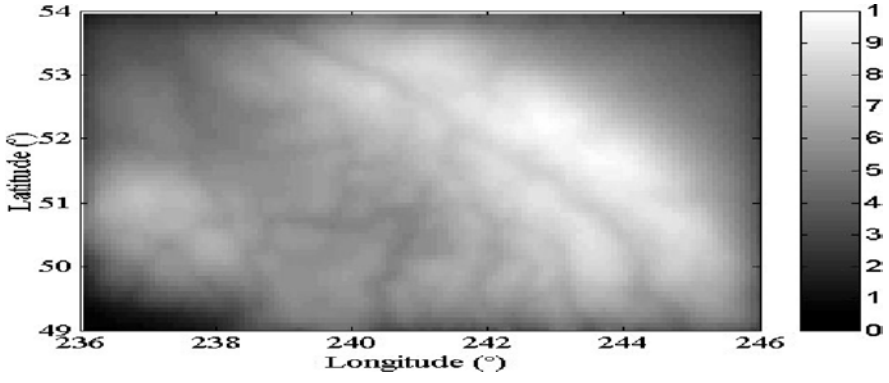

Fig. 12. Indirect effect on the geoid for the Pratt-Hayford model (m)

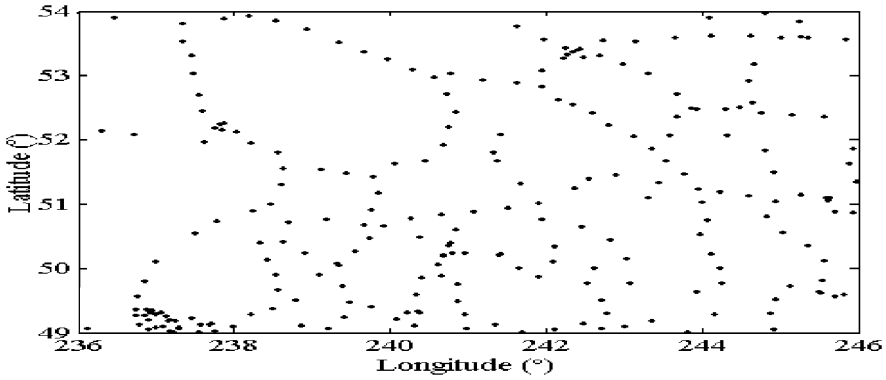

Fig. 13. Distribution of GPS-leveling points in the test area

Table 3. Statistics of different gravimetric geoid solutions (m)[a]

Reduction scheme	Max	Min	Mean	Std
Rudzki	0.76 (1.37)	−0.56 (0.12)	0.00 (0.67)	0.19 (0.35)
Helmert	0.62 (1.97)	−0.59 (0.65)	0.00 (1.33)	0.19 (0.23)
RTM	0.76 (1.46)	−0.55 (0.31)	0.00 (0.77)	0.19 (0.21)
Airy–Heiskanen	0.59 (−4.85)	−0.86 (−6.64)	0.00 (−5.64)	0.26 (0.35)
Pratt–Hayford	0.54 (−5.18)	−0.81 (−6.81)	0.00 (−5.77)	0.25 (0.34)

[a]Values in the parentheses are before fit.

5 Conclusions

This paper shows the importance of studying other gravimetric reduction schemes both in theory and in practice in the context of precise geoid determination, in addition to the usual Helmert's second method of condensation and the RTM method. Rudzki anomalies have smaller standard deviation and range than those of Helmert anomalies. Helmert anomalies yield the roughest gravity field in the test area, while topographic–isostatic anomalies with AH and PH models produce a smoother field, as well as less correlation with topography. The removal of the EGM96 contribution does not improve the statistics of the AH and PH anomalies but does improve those of the Helmert and Rudzki anomalies because Helmert and Rudzki gravity anomalies possess statistics similar to those of FA anomalies.

The indirect effect of topographic–isostatic reductions on geoid undulations reaches 10 m, while the indirect effect of Helmert's method is only 47 cm. The maximum restored terrain effect on the quasigeoid for the RTM reduction is nearly 1 m.

The Rudzki geoid performs as well as the Helmert and RTM geoids, and better than the AH and PH geoids compared to GPS-leveling. It has the smallest bias among all other reduction schemes. The Rudzki reduction is, therefore, a viable tool for gravimetric geoid determination in mountainous regions. The main advantage of using this method is that we do not have to deal with the computational burden of the indirect effect on the geoid, which is required for the other reduction schemes. On the other hand, the Helmert and RTM methods require not only the computation of indirect effects on the geoid and restored terrain effects on the quasigeoid, respectively, but also some additional computations; in Helmert's second method of condensation, we need to use different reduction methods for smooth gravity interpolation, while in the RTM reduction the transformation from quasigeoid to geoid is required for geoid determination. More practical studies using the Rudzki inversion scheme (not only in planar, but also in spherical approximation) should be carried out in different parts of the world, especially in areas of high mountains. The large bias in the topographic–isostatic geoid solutions indicates that we should use a corresponding topographic–isostatic geopotential model to extract the low-frequency part of the gravity signal.

Acknowledgments. This research has been supported by grants to the second author from the Geomatics for Informed Decisions (GEOIDE) Network of Centers of Excellence (NCE) and the Natural Sciences and Engineering Research Council of Canada. The authors are grateful to the reviewers for their constructive comments that have resulted in a much-improved manuscript.

References

Abd-Elmotaal HA, Kühtreiber N (2003) Geoid determination using adapted reference field, seismic Moho depths and variable density contrast. J Geod 77:77–85

Bajracharya S (2003) Terrain effects on geoid determination. MSc thesis, rep 20181, Department of Geomatics Enginering, University of Calgary

Forsberg R (1984) A study of terrain reductions, density anomalies and geophysical inversion methods in gravity field modeling. Rep 355, Department of Geodetic Science and Surveying, The Ohio State University, Colombus

Haagmans R, de Min E, van Gelderen M (1993) Fast evaluation of convolution integrals on the sphere using 1D FFT and a comparison with existing methods for Stokes' integral. Manuscr Geod 18:227–241

Heck B (1993) A revision of Helmert's second method of condensation in geoid and quasigeoid determination. IAG Symp 112. Springer, Berlin Heidelberg New York, pp246–251

Heck B (2003) On Helmert's methods of condensation. J Geod 77:155–170

Heiskanen WA, Moritz H (1967) Physical geodesy. Freeman, San Fransisco

Heiskanen WA, Vening Meinesz FA (1958) The earth and its gravity field. McGraw-Hill, New York

Kellogg OD (1929) Foundations of potential theory. Springer, Berlin Heidelberg New York (reprinted by Dover, New York, 1953)

Kuhn M (2003) Geoid determination with density hypotheses from isostatic models and geological information. J Geod 77:50–65

Lambert WD (1930) The reduction of observed values of gravity to sea level, Bull Géod 26:107–181

Lemoine FG, Kenyon SC, Factor JK, Trimmer RG, Pavlis NK, Chinn DS, Cox CM, Klosko SM, Luthcke SB, Torrence MH, Wang YM, Williamson RG, Pavlis EC, Rapp RH, Olson TR (1998) The development of the joint NASA GSFC and the National Imagery and Mapping Agency (NIMA) geopotential model EGM96. *NASA/TP-1998–206861*, National Aeronautics and Space Administration, Maryland

Macmillan WD (1958) The theory of the potential. Dover, New York

Pellinen LP (1962) Accounting for topography in the calculation of quasigeoidal heights and plumbline deflections from gravity anomalies. Bull Géod 63:57–65

Nagy D (1966) The prism method for terrain corrections using digital computers. Pure Appl Geophys 63:31–39

Rudzki MP (1905) Sur la determination de la figure de la terre dapres les mesures de la gravite. Bull Astron Ser B22:1905

Sideris MG (1990) Rigorous gravimetric terrain modeling using Molodensky's operator. Manuscr Geod 15:97–106

Vanicek P, Martinec Z (1994) The Stokes–Helmert scheme for the evaluation of precise geoid. Manuscr Geod 19:119–128

Wang YM, Rapp RH (1990) Terrain effects on geoid undulations. Manuscr Geod 15:23–29

Wichiencharoen C (1982) The indirect effects on the computation of geoid undulations. Rep 336, Department of Geodetic Science and Surveying, The Ohio State University Columbus